Estuaries and Coasts (2024) 47:2267–2282
https://doi.org/10.1007/s12237-024-01407-x

Spatial and Temporal Variability of Century-Scale Sediment Accumulation in an Active-Margin Estuary

Emily Eidam[1,2] · T. Souza[2] · M. Keogh[3] · D. Sutherland[3] · D. K. Ralston[4] · J. Schmitt[5] · A. Helms[5]

Received: 20 October 2023 / Revised: 25 June 2024 / Accepted: 13 July 2024 / Published online: 10 August 2024

Abstract

Estuaries worldwide have been altered by anthropogenic modifications including land clearing, dredging, and land reclamation, which impact sediment routing and accumulation on tidal flats. Numerous studies have explored tidal flat and marsh vulnerability to submergence or "drowning" under accelerating sea-level rise, but recent work along the Oregon coast suggests estuaries are maintaining positive accretionary balances (at least in marshes) despite ongoing sea-level rise. In this study, accretion rates (sediment accumulation rates) were evaluated from ^{210}Pb profiles at eight sites on broad intertidal flats in Coos Bay, one of the largest estuaries on the U.S. West Coast and a site of substantial development and logging since the mid-1800s. Based on the century-scale record of sediment accretion represented by ^{210}Pb profiles, tidal flats have been accreting at rates of ~ 1–3 mm/yr with little spatial relationship to relative sea-level rise or patterns of tectonic uplift. Thus, accretion is generally not accommodation- or supply-limited, and therefore likely not regulated by sea-level rise. Peaks in sediment accretion are well-preserved from the last 30 years, and accretion rates averaged over this more modern time span tend to be four times greater than rates averaged over the whole-core (century-scale) ^{210}Pb records. It is unclear whether the higher, more modern rates represent a real change in estuarine accretion patterns over the past decades or a Sadler effect (i.e., an apparent but not real increase in accretion in younger sediments). The results highlight the spatial variability in accretion rates within a single estuary, the potential resiliency of this tectonically active estuary to sea-level rise (in the form of a positive accretionary balance), and raise the issue of whether management decisions are best made based on century-scale accretion rates or multi-decadal accretion rates.

Keywords Estuary · Sediment accumulation · Geochronology · Sea-level rise · Tidal flat

Introduction

Increased rates of eustatic sea-level rise during the Anthropocene have prompted growing concern about some salt-marshes and intertidal flats "drowning," meaning that areas which are presently intertidal may become subtidal (or may become submerged for longer periods of time each day or fortnight), with impacts for ecological services (Breda et al. 2021; Kirwan and Megonigal 2013; Thorne et al. 2018). Sediment supply is a primary driver of vertical accretion in many estuaries; when sediment supplies are high, tidal flats accrete rapidly at rates outpacing the creation of accommodation space through relative sea-level rise (RSLR; e.g., Thorne et al. 2018). Anthropogenic activities in adjacent watersheds such as land clearing for timber or agriculture can increase sediment supplies and promote resilience of intertidal areas (e.g., Gunnell et al. 2013; Rodriguez et al.

Communicated by Meagan Eagle

✉ Emily Eidam
Emily.eidam@oregonstate.edu

1 College of Earth, Ocean, and Atmospheric Sciences, Oregon State University, Corvallis, OR, USA

2 Department of Earth, Marine, and Environmental Sciences, University of North Carolina at Chapel Hill, Chapel Hill, NC, USA

3 Department of Geological Sciences, University of Oregon, Eugene, OR, USA

4 Woods Hole Oceanographic Institute, Woods Hole, MA, USA

5 South Slough National Estuarine Research Reserve, Charleston, OR, USA

2020), while cessation of these activities or damming can reduce sediment supplies and lead to increased submergence of flats and marshes that had expanded as a result of anthropogenic landscape disturbance (e.g., Noe et al. 2020).

Within an estuary, other developments such as dredging or shoreline hardening can alter estuarine hydrodynamics and thus alter patterns of sediment delivery, deposition, and erosion beyond what a change in supply can accomplish. In some cases, these developments reduce the amount of sediment transferred to intertidal flats, thus slowing accretion rates (van Dijk et al. 2021). When these changes are combined with climate shifts (e.g., changing precipitation patterns) and superimposed on regional geologic processes (e.g., tectonic uplift), the result is variable records of sediment accumulation even within a single estuary, which can confound efforts to project future tidal flat accretion. In this study, we explore temporal and spatial variability in sediment accumulation within the Coos Estuary in Oregon. Sediment accumulation (accretion) in this estuary has been impacted by multiple perturbations in the last century including timber harvests, dredging, land reclamation, and tectonic uplift, and in the past few centuries by tectonic subsidence related to a year 1700 earthquake (e.g., Percy et al. 1974; Borde et al. 2003; Ivy 2015; Burgette et al. 2009; Nelson et al. 1998), making it a valuable study site for best practices in evaluating tidal flat accretion history from sediment cores. Based on hydrodynamic and sediment modeling of the estuary, dredging and reclamation projects have increased net sediment retention through changes in hydrodynamics independent of any changes in sediment supply (Eidam et al. 2021), but this has not been validated through observational sedimentary records.

To assess the impacts of these types of perturbations on sediment accretion in the Coos Estuary and assess century-scale changes in accretion, sediment accumulation rates (SARs) and mass accumulation rates (MARs) were assessed using cores spanning the estuary from the mouth to the freshwater zone. Rates were calculated for each core interval using an age model, and then depth-averaged rates were calculated using a weighted mean for the entire core as well as the most recent 30-year periods to assess how the time-scale of analysis impacts the accretion-rate estimates. This research (1) illustrates how different regions of the estuary respond to watershed and estuary disturbances, (2) explores whether sea-level rise exerts a major control on accretion in this tectonically active estuary, and (3) explores what time-scale of averaging is suitable for interpretations of mean accretion rate. Estuarine wetlands are critical environments for human economies and natural ecosystems; understanding their behavior to different perturbations is key to maintaining and restoring healthy estuaries and predicting future trajectories of sediment accretion.

Regional Setting

The Coos Estuary encompasses 54 km^2 (Rumrill 2007) and is the largest estuary between the Columbia River and San Francisco Bay (Fig. 1). Large estuaries are sparse in this region due to tectonic uplift, which forms small, steep watersheds characterized by high sediment yields and episodic seismic activity. Coos Bay has been developed as a port for fishing and timber export since the mid-nineteenth century

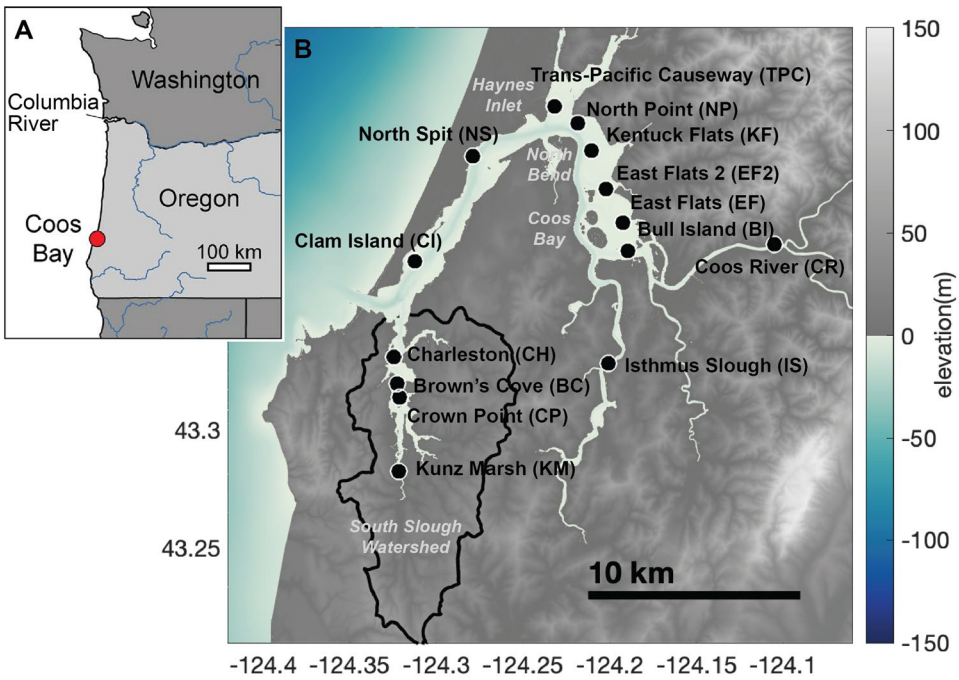

Fig. 1 Map of coring locations and regional context. **A** Location of Coos Bay on the Oregon Coast. **B** Coring locations within Coos Bay. The black outline denotes the South Slough Watershed

resulting in an extensive history of modification, especially in the last ~ 150 years (Borde et al. 2003; Ivy 2015; Johnson et al. 2019; Eidam et al. 2021). The South Slough National Estuarine Research Reserve, established in 1974, protects 26 km^2 of the watershed from development (Rumrill 2007; Fig. 1).

The main part of the estuary is the horseshoe-shaped drowned river valley of the Coos River, which includes broad intertidal sand and mud flats as well as a dredged channel (> 11 m deep) on the east side, and a single deep channel bordered by narrower tidal flats on the west side (Fig. 1; Maddin 1995). South Slough is a shallow subembayment near the mouth of the estuary with a maximum depth of ~ 5.5 m. In the main channel, tidal amplitudes range from ~ 1.4 to 2.5 m (Eidam et al. 2020). Coos Bay and South Slough receive fresh water from ~ 30 small streams and rivers (Coos Watershed Association, https://cooswatershed.org/) that receive high rainfall during winter storms and atmospheric river events (Saldías et al. 2020). Discharge from the Coos River (the largest freshwater source) varies seasonally from 1 m^3/s in the summer to > 300 m^3/s in the winter. Local watersheds are characterized by low forested hills, which have been the site of an active timber industry that peaked in the 1970s when > 80% of the drainage basin was under management for timber harvest (Percy et al. 1974). Some logging continues today (Port of Coos Bay, 2018).

Rates of relative sea-level rise are low and variable due to ongoing tectonic uplift. Based on tide gauge data, the mean RSLR rate at Charleston (Fig. 1B) was 0.98 ± 0.64 mm/yr between 1970 and 2022 (NOAA 2022). Uplift rates throughout Coos Bay and South Slough range from 0.61 to 1.94 mm/yr (Burgette et al. 2009; Fig. 2A). Based on the rate of RSLR at Charleston and nearby measured uplift rates (each < 1 km east or west of the Charleston tide gauge) of 1.99 and 2.03 mm/yr, the rate of eustatic sea-level rise (SLR) at Charleston is assumed to be 2.99 mm/yr (0.98 mm/yr + 2.01 mm/yr). To obtain approximate RSLR rates throughout the estuary, the uplift rates provided by Burgette et al. (2009) were subtracted from the calculated SLR rate of 2.99 mm/yr at Charleston (Fig. 2B).

The most recent large seismic event (the Cascadia Earthquake, 1700) generated a tsunami, approximately 1 m of subsidence, and deposition of sand within the estuary (Nelson et al. 1998; Hawkes et al. 2011). This event may have caused the extirpation of native Olympia oyster (*Ostrea lurida*), which continues to have low and unstable population numbers despite restoration efforts (Groth and Rumrill 2009). In the present day, reefs and oyster aquaculture supporting non-native *Crassostrea gigas* oysters occur throughout the estuary and prominent eelgrass (*Zostera marina*) beds occur on tidal flats from the mouth of the estuary to North Bend and in South Slough (Groth and Rumrill 2009; Rumrill and Sowers 2008). In recent years, declining populations have generated interest in the impacts of sediment accretion on populations of native oysters and eelgrass in Coos Bay (Rumrill and Sowers 2008; Anderson 2020).

Prior to estuary development, the Coos River intersected the bay as a network of distributary channels across the broad eastern tidal flats. Dredging projects rerouted the river mouth to connect more directly with the main navigation channel starting in the early 1900s (see Eidam et al. 2020). The main channel continues to be dredged (USACE, 2015). River rerouting, dredging, and reclamation of intertidal areas through dredge spoil disposal and infrastructure projects have impacted the hydrodynamics, tidal range, and sediment

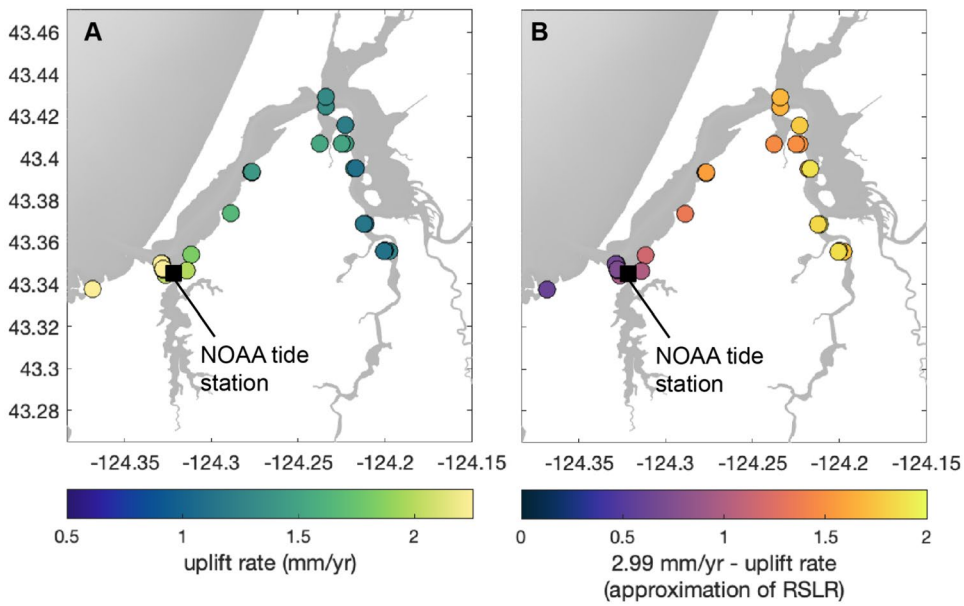

Fig. 2 Uplift rates and RSLR rates in the Coos Bay region. **A** Uplift rates across Coos Bay (Burgette et al. 2009). **B** Corresponding approximate RSLR rates for the Coos Bay Region

dynamics in the estuary. The estuary turbidity maximum (ETM) has strengthened, deposition in the navigation channel has increased, and more sediment is now delivered to the northern end of the east flats because of changes in the ETM dynamics (Eidam et al. 2020, 2021). Based on model results (Eidam et al. 2021) and four cores collected in marginal areas (in South Slough and Haynes Inlet; Mathabane 2015 and Johnson et al. 2019), these changes may be related to an increase in net sediment retention, though spatial variability in sediment accretion trends is not well-constrained.

Methods

Core Collection and Analyses

In May 2021, 14 cores of ~ 12–100 cm in length were collected from shallow subtidal areas and intertidal flats across Coos Bay (Fig. 1; Table 1). Subtidal cores were collected using a 10-cm diameter push coring device operated by hand from a boat. Tidal flat cores were collected using a 6-cm diameter Russian peat corer. Compaction during collection

Table 1 Coring site characteristics and analyses performed on each core (Pb, ^{210}Pb activity; GS, grain size; LOI, loss-on-ignition; analyses were performed on selected intervals as noted in results figures in the text and supplemental)

Site name	Site description	Vegetation presence	Lon	Lat	Distance up-estuary from jetties (km)	Water depth relative to mean sea level, NAD 83 datum (m)	Analyses
South Slough							
Charleston (CH)	Tidal flat; shell debris, sandy mud	Dense eelgrass nearby	− 124.324	43.331	4.4	1.2	Pb, GS, LOI
Brown's Cove (BC)	Tidal flat	Sparse eelgrass, much *Ulva*; cored in bare area	− 124.323	43.320	5.0	1.3	Pb, GS, LOI
Crown Point (CP)	Tidal flat	No eelgrass	− 124.321	43.314	6.53	2.1	Pb, GS
Kunz Marsh (KM)	Unvegetated tidal flat	Algae, no eelgrass	− 124.322	43.283	8.92	1.8	Pb, GS, LOI
Coos Bay							
Clam Island (CI)	Sandy flat, clams nearby	Dense eelgrass in vicinity	− 124.312	43.371	3.50	1.4	
North Spit (NS)	Small, sandy flat	Dense algae	− 124.279	43.416	9.35	1.7	
Trans-Pacific Causeway (TPC)	Subtidal core on submerged flat; very soft sediment	No vegetation detectable from vessel	− 124.232	43.437	13.6	1.4	GS, LOI
North Point (NP)	Subtidal core on sandy submerged flat	No vegetation detectable from vessel	− 124.219	43.430	14.2	1.9	
Kentuck Flats (KF)	Large tidal flat; cored near small inlet channel	Areas of dense eelgrass in vicinity	− 124.210	43.418	15.4	1.5	Pb, GS
East Flats 2 (EF2)	Subtidal core near areas of oyster aquaculture in middle of large eastern flats	No vegetation detectable from vessel	− 124.202	43.402	18.0	1.8	Pb, GS, LOI
East Flats (EF)	Subtidal core on edge of flat near the pre-dredging main river channel	Algae on surface of core	− 124.192	43.388	19.8	1.4	GS
Bull Island (BI)	Large, muddy tidal flat	No vegetation	− 124.190	43.376	22.1	0.62	Pb, GS, LOI
Isthmus Slough (IS)	Muddy tidal flat with abundant woody debris	Minor algae, no eelgrass	− 124.201	43.328	26.6	1.4	Pb, GS, LOI
Coos River (CR)	Small tidal flat alongside river channel	Bare mud	− 124.105	43.378	30.6	2.2	GS, LOI

was considered minimal because a Russian peat corer was used at most sites (which samples sediments using a split soon, which causes little to no compaction) and push cores were relatively short (see further discussion in Supplemental Section D). Cores collected using a Russian peat corer were subsampled in 1-cm increments in the field and combined with a second core collected within a 30-cm radius of the first core to ensure sufficient material for analyses. All cores were subsampled into 1-cm increments and analyzed for porosity, dry bulk density, grain-size distributions, and organic content. Eleven cores that had sufficient fine-grained sediment were also analyzed for ^{210}Pb activities, and eight of these yielded useful profiles (the remaining three were heavily mixed; see the "Results" section).

Subsamples were weighed, freeze-dried for > 48 h to ensure complete dryness, and reweighed to determine porosity and dry bulk density. Approximately 50% of each sample was saved as unseparated bulk material and was analyzed for grain-size distributions using a laser diffraction particle sizer, and for organic content using a loss-on-ignition (LOI) procedure (samples were combusted in glass vials in a muffle furnace at 550 °C for 5 h; weighing and desiccation were conducted pre- and post-combustion). The remaining 50% of each sample was hand-sieved to obtain the fine fraction (< 63 μm) that was used for radioisotope analysis.

^{210}Pb Dating, Interpolation, and Age Modeling

Total activities of ^{210}Pb from eleven cores were measured using an acid digestion and alpha spectroscopy procedure at the University of North Carolina at Chapel Hill (e.g., Nittrouer et al. 1979). Selected subsamples (from 1-cm sections cut in the field) were dried and sieved at 63 μm, and ~ 1.5 g of fine-grained material (silts and clays) was used for analyses. (The topic of grain size in relation to ^{210}Pb activities is well-addressed by He and Walling 1996 and Zhang et al. 2023) Initially, subsamples were selected at 5-cm intervals down-core, but some additional samples were also analyzed from areas of interest such as the top and bottom of the cores and areas of apparently rapid accumulation within each core. To improve data density, ^{210}Pb activities were interpolated between measured intervals using the exponential interpolation equation described by Appleby (2001).

Within the seabed, the total activity of ^{210}Pb decays from a high concentration at the surface to a background or "supported" in sediments older than ~ 125 years (the depth to this zone is called the "depth to background" of the core; Brush et al. 1982). In this study, we used the minimum ^{210}Pb value below the zone of decay as the supported ^{210}Pb value (see Table 2). It is worth noting that some researchers use ^{226}Ra (measured using gamma spectroscopy) as a proxy for supported ^{210}Pb, because the two isotopes are in secular equilibrium below the zone of ^{210}Pb decay. However, this approach is problematic because ^{210}Pb activities measured by alpha spectroscopy represent the isotope present on particle surfaces (or surface coatings), whereas gamma spectroscopy measures decay of isotopes on particle surfaces and within the mineral matrix itself—and thus, gamma-derived values supported ^{210}Pb activity are expected to be systematically higher than alpha-derived values (e.g., Nittrouer et al. 1979; Zaborska et al. 2007). However, using ^{226}Ra is advantageous if there is ambiguity about whether the core length exceeds the depth to background (i.e., if there is concern that there is still excess ^{210}Pb present throughout the core). In this study, one to two samples per core from different depths (e.g., near the surface and near the bottom of the core) were analyzed for ^{226}Ra activities using gamma spectroscopy in broad-energy Germanium (BEGe) well detectors. While the ^{226}Ra activities were systematically higher than supported ^{210}Pb values measured from the alpha process (Supplemental Table S1), the ^{226}Ra values (from gamma spectroscopy) and supported ^{210}Pb values (from alpha spectroscopy) exhibited a linear relationship for all cores (Supplemental Fig. S1), suggesting that the core lengths did indeed exceed the depth to background, and use of the minimum ^{210}Pb activity below the zone of decay as the supported value is a valid choice.

To calculate isotope inventories and sediment mass accumulation rates, excess ^{210}Pb values (i.e., the total ^{210}Pb activity minus the supported ^{210}Pb activity) were assumed to represent a homogenous value within each subsample interval. Total areal dry mass for the interval was then calculated from the dry bulk density to obtain the interval inventory of ^{210}Pb (see Sanchez-Cabeza and Ruiz-Fernandez, 2012). In some cores, the surface interval of the core (0–1 cm) provided insufficient fine sediment for analysis due to a large fraction of coarse sediments (i.e., sands). In these cases, the surface activity of the core was interpolated using a linear estimation from the four measured (non-interpolated) values closest to the surface.

Age modeling for the cores was performed using the Constant Flux (CF) model (which originated as the Constant Rate of Supply model; see Appleby and Oldfield 1978; Appleby 2008; Sanchez-Cabeza and Ruiz-Fernandez, 2012; Arias-Ortiz, 2018). This model was selected because the assumptions of the Constant Activity or Constant Incoming Concentration model (Robbins 1978) and Constant Flux, Constant Sedimentation model (Krishnaswamy et al. 1971) were not met in this estuary due to (1) varying sediment accretion rates or bioturbation (see Results) and (2) varying salinities throughout the period of interest (see Eidam et al. 2020). To obtain a long-term mean sediment accretion rate, the annual SARs obtained from the CF model were averaged over the entire core as well as over the most recent 30 years of the sedimentary record (which may be more

Table 2 Sediment grain-size characteristics and weighted-mean accumulation rates from cores. Note that percent differences in the right-most column have been signed to indicate an increase or decrease in the parameter through time

(A) Site	(B) Depth-averaged d_{50} (um), entire profile	(C) Supported activity (dpm/g)	(E) Water depth (m)*	(E) SAR (mm/yr), entire profile (CF)	(F) SAR (mm/yr), last 30 yrs (CF)	(G) MAR (g/cm^2/yr), entire profile (CF)	(H) % difference in SAR, (F) versus (E)	(I) Nearest RSLR estimate (mm/yr)	(J) (E) minus (I) (mm/yr)	(K) (F) minus (I) RSLR (mm/yr)
South Slough										
Charleston (CH)	171	0.86	1.2	1.1 ± 0.051	0.48 ± 0.0013	2.1 ± 0.070	−82%	0.96	0.14	−0.48
Brown's Cove (BC)	74.6	0.47	1.3	2.0 ± 0.14	9.1 ± 0.95	4.6 ± 0.21	128%	0.96	1.04	8.1
Crown Point (CP)	69.6	1.32	2.1	2.0 ± 0.12	6.6 ± 0.65	8.3 ± 0.29	108%	0.96	1.04	5.6
Kunz Marsh (KM)	25.5	0.73	1.8	2.9 ± 0.24	8.3 ± 0.78	4.4 ± 0.32	96%	0.96	1.94	7.3
Coos Bay										
Trans-Pacific Causeway (TPC)	115	-	1.4	-	-	-	-	1.68	-	-
Kentuck Flats (KF)	86.9	1.0	1.5	2.5 ± 0.056	5.7 ± 0.15	5.2 ± 0.088	78%	1.78	0.72	3.9
East Flats 2 (EF2)	104	1.1	1.8	1.4 ± 0.061	4.0 ± 0.13	4.7 ± 0.24	95%	1.89	-0.49	2.1
East Flats (EF)	91.2	-	1.4	-	-	-	-	1.89	-	-
Bull Island (BI)	51.5	0.48	0.62	2.7 ± 0.23	4.2 ± 0.17	5.5 ± 0.45	45%	1.73	0.97	2.5
Isthmus Slough (IS)	23.4	0.52	1.4	1.3 ± 0.065	2.1 ± 0.03	1.0 ± 0.052	45%	1.87	-0.57	0.23
Coos River (CR)	26.0	-	2.2	-	-	-	-	1.73	-	-

*Note that all sites are deeper than 0.5 m; depths are relative to mean sea level (NAD 83 datum)

relevant to modern management applications). This averaging was done using a weighted approach: for each interval, the SAR for that interval was multiplied by the time frame represented by that interval. The results were summed and divided by the total amount of time represented by all intervals considered.

Results

Grain Size

Grain-size distributions varied spatially across the Coos Estuary, as well as vertically within some cores (representing temporal variation; Table 2, Fig. 3). Spatially,

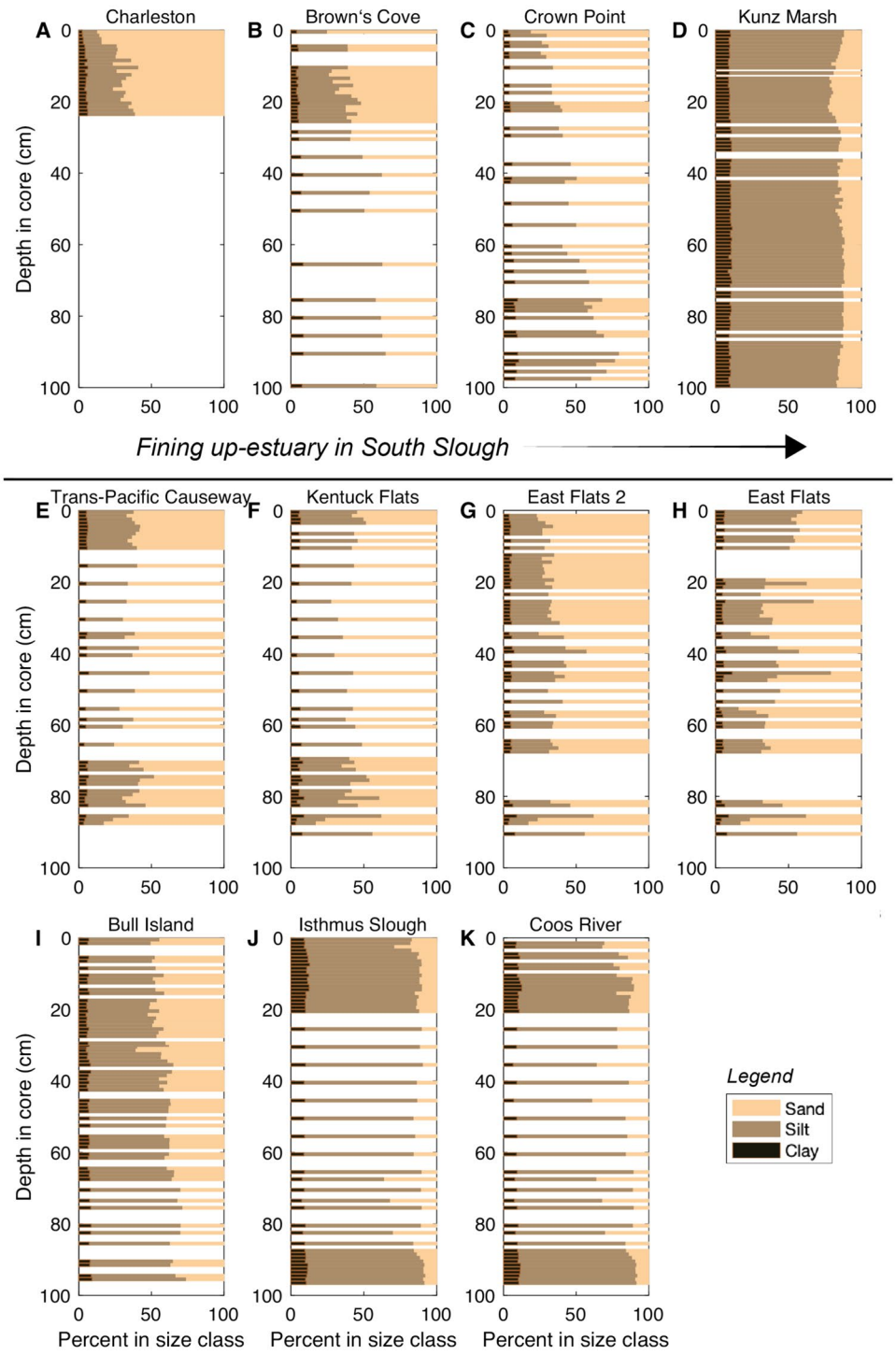

Fig. 3 Down-core clay/silt/sand fractions for 11 sites illustrated in Fig. 1. **A** Charleston. **B** Brown's Cove. **C** Crown Point. **D** Kunz Marsh. **E** Trans-Pacific Causeway. **F** Kentuck Flats. **G** East Flats 2. **H** East Flats. **I** Bull Island. **J** Isthmus Slough. **K** Coos River. Sites are arranged by South Slough in the top row (seaward to landward) and the main estuary in the bottom two rows (also seaward to landward). In both South Slough and the main estuary, there is a general trend of fining in the landward direction (e.g., finer sediments occur near river sources). Some cores exhibited down-core trends in grain size (i.e., temporal variability)

sediments coarsened seaward (Fig. 3). Depth-averaged median grain sizes (d_{50}) ranged from ~ 23–25 µm (silt) at Isthmus Slough and Kunz Marsh in the upper estuary to ~ 170 µm (fine sand) at Charleston near the estuary mouth (Table 2).

Sediment sizes at most sites coarsened through time. Isthmus Slough and Kunz Marsh, which are fine-grained sites (dominantly silt), exhibited a 19–35% increase in depth-averaged d_{50} between 1880–1910 and 1990–2021 (Fig. 3). Mixed sand/silt sites exhibited 13–101% increases in depth-averaged d_{50}, except for Kentuck Flats which exhibited an 11% decrease.

Organic Content

Organic matter fractions assessed using loss-on-ignition (LOI) were relatively low across the estuary and varied spatially (together with grain size) along the freshwater to marine gradient. Sites with coarser sediments near the marine end (North Spit, Charleston, Crown Point) displayed organic fractions as low as 0.01 (or 1%; Fig. 4). Conversely, sites with finer sediments closer to freshwater inputs (Kunz Marsh, Catching Slough, Isthmus Slough) displayed higher fractions (~ 0.08–0.15). In several cores, peaks in organic content coincided with woody debris layers. The presence of eelgrass in the vicinity of some cores did not appear to correspond to variations in organic content—unvegetated mid-estuary sites such as Bull Island had organic values comparable to vegetated mid-estuary sites such as Trans-Pacific Causeway (though cores were not collected in eelgrass beds; see Table 1, Fig. 4).

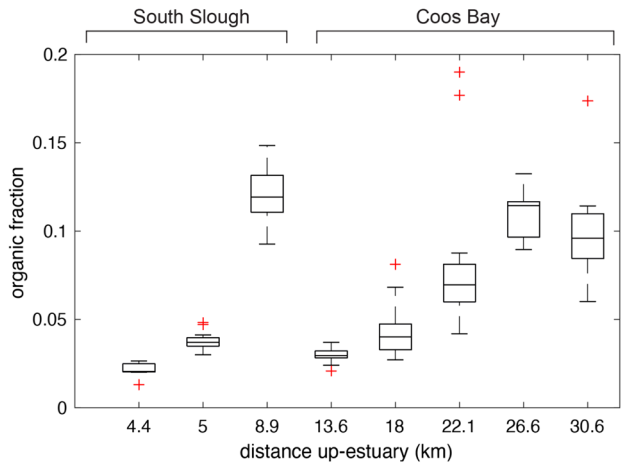

Fig. 4 Spatial distribution of organic fraction results. Each box-and-whisker plot represents all intervals that were analyzed in a single core. On a site-by-site basis, organic content generally increased up-estuary (both in South Slough and in Coos Bay)

^{210}Pb Activity Profiles and Sediment Accumulation Rates

Of the 14 cores collected from across the Coos Estuary, 11 had sufficient fine-grained sediment to warrant isotope analyses (i.e., at least 1 g of dried, fine-grained sediment < 63 µm in size per 1-cm subsample). Three of these cores (Trans-Pacific Causeway, East Flats, and Coos River) exhibited extensive mixing or disturbance within the cores and were not used for accumulation-rate analyses because of distortions in the ^{210}Pb profiles. High levels of disturbance and problems creating geochronologies in tidal-flat samples have been noted in other Oregon estuaries (Peck et al. 2020). The remaining eight cores exhibited wide variations in ^{210}Pb activities, depths to background, and sediment accumulation rates (see detailed results in Figs. S2–S11).

Total ^{210}Pb activities were typically less than 5 dpm/g (Fig. S2), which is comparable to or somewhat lower than values obtained in other estuaries in this region (e.g., Boldt et al. 2013; Peck et al. 2020). (Note that activities are reported in dpm/g as is common in the literature; these values can be converted to Bq/kg using the factor of 1 Bq = 60 dpm.) Background activities (generated by in situ ^{210}Pb production from decay within minerals) were interpreted to be 0.47 to 1.3 dpm/g based on ^{210}Pb activities below the region of ^{210}Pb decay (see the "^{210}Pb Dating, Interpolation, and Age Modeling" section and Table 2), and excess ^{210}Pb activities ranged from 0 to 4 dpm/g (Fig. S3; Eidam et al. 2023). In general, surficial ^{210}Pb activity was greater at sites of higher salinity (sites closer to the estuary mouth), as is expected due to the low atmospheric flux of ^{210}Pb to this region and the relatively high marine ^{210}Pb activities in the Northeast Pacific (Carpenter et al. 1981; Zhang et al. 2021).

The shapes of excess ^{210}Pb decay profiles and calculated SARs and MARs were variable among cores (Figs. S2–S11). Some cores exhibited peaks in excess ^{210}Pb activity at multiple depths (e.g., Brown's Cove, Bull Island, Kentuck Flats, and especially Crown Point; Fig. S3). Other sites exhibited a very shallow depth to background (e.g., Charleston and Isthmus Slough). Kunz Marsh exhibited variable ^{210}Pb in the upper 20 cm which was interpreted as evidence of mixing (Fig. S3H). Crown Point exhibited an anomalous peak at ~ 68 cm depth (Fig. S2D). In all cores, however, there was an obvious isotope decay signal with depth.

The CF age model yielded interval-by-interval SARs ranging from 0 to more than 30 mm/yr and MARs ranging from 0 to more than 20 g/cm^2/yr (Figs. S4–S11). The weighted-mean SARs from entire profiles (dating back to the 1800s) ranged from 1.1 ± 0.051 to 2.9 ± 0.24 mm/yr, and the weighted-mean MARs ranged from 1.0 ± 0.052 to 8.3 ± 0.29 g/cm^2/yr.

Sediment (and mass) accumulation rates varied spatially. For example, the core collected from a small tidal flat in

Isthmus Slough (far from the estuary entrance) had a slow mean accretion rate of ~ 1.3 mm/yr (Table 2, Fig. S9). The Charleston core, collected near the estuary mouth, exhibited a similarly slow accretion rate of ~ 1.1 mm/yr (Fig. S6), as did the East Flats 2 core from the broad intertidal flats in the middle estuary. The highest accretion rates (2.7–2.9 mm/yr) occurred at Kunz Marsh and Bull Island, which are both near riverine sources of sediment. However, Kentuck Flats in the middle estuary also exhibited a high mean accretion rate (2.5 ± 0.056 mm/yr). Thus, despite high SARs occurring near riverine sources, there was no clear relation between SARs and distance from the estuary entrance (or water depth; Fig. S15). Patterns of mass accumulation rates (MARs) generally followed patterns of SARs—Brown's Cove and Crown Point had the highest MARs, while Charleston and Isthmus Slough had the lowest MARs (Table 2, Figs. S4–S11).

Notable peaks in accumulation rate were observed at all sites except Charleston and Isthmus Slough (Fig. 5). Most of these peaks occurred within the past 30 years, and each represented a few years of increased sediment accretion (Fig. 5C, D). Peaks in SARs in South Slough were generally larger (20–40 mm/yr) than in Coos Bay (5–18 mm/yr).

SARs averaged over the last 30 years of the ^{210}Pb decay profiles were generally two to four times higher than values averaged over the entire profiles (~ 120–160 years), a result which reflected the presence of sediment accretion peaks in the more recent part of each record (Table 2, Fig. 5C, D, Figs. S4–S11). Brown's Cove and Crown Point exhibited the greatest differences in accumulation rate between modern and long-term periods (+ 108 to 128%), and even Isthmus Slough (a slow-accumulation site) exhibited a + 45% difference. Charleston was the one exception to the trend and

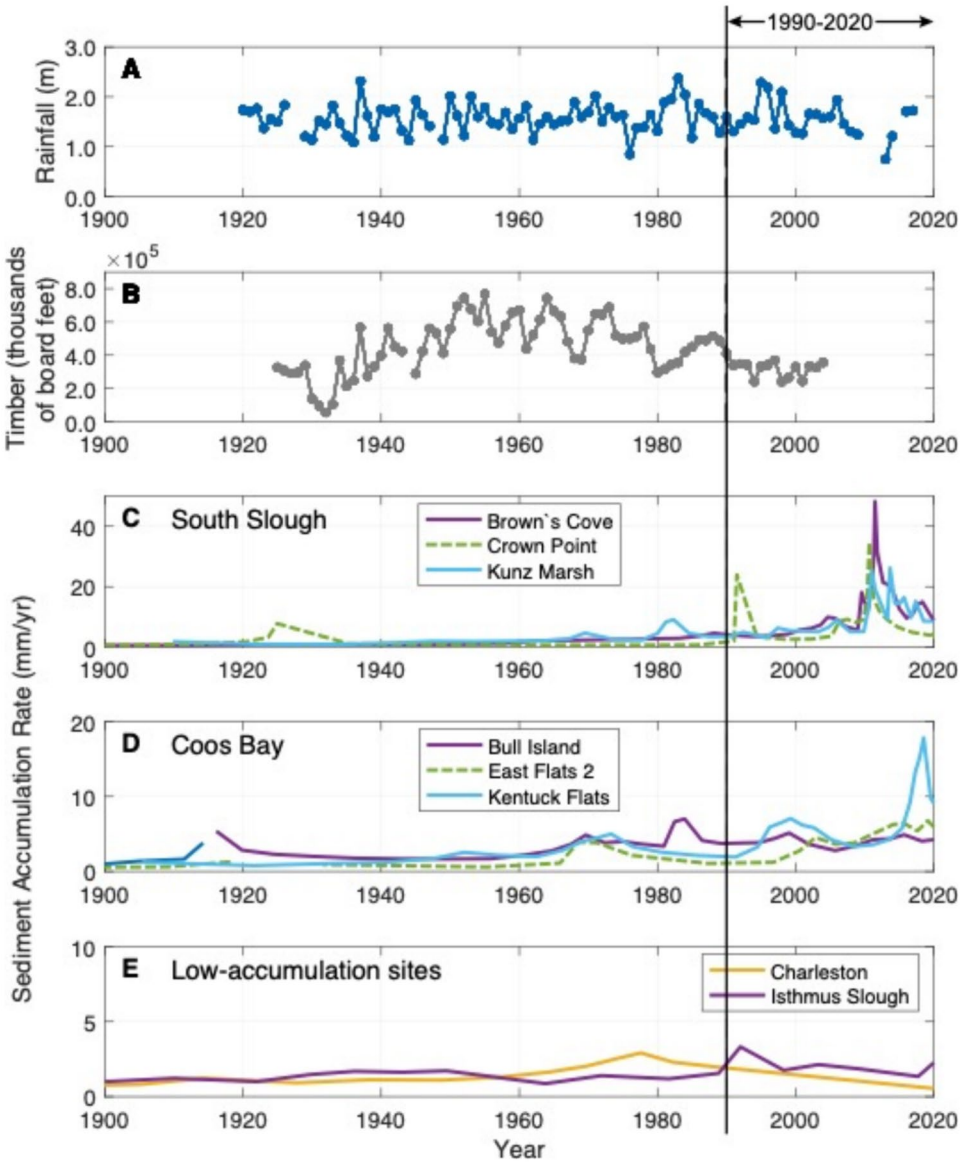

Fig. 5 Rainfall totals, timber harvest, and sediment accretion records for the past ~ 125 years. (**A**) Annual total precipitation at North Bend (from NOAA, www.weather.gov/wrh/Climate). (**B**) Timber harvest in Coos County in thousands of board feet per year (from Andrews and Kutara 2005). (**C**) Accretion rates at rapidly accumulating sites in South Slough. (**D**) Accretion rates at rapidly accumulating sites in Coos Bay. (**E**) Accretion rates at slowly accumulating marginal flats (Charleston and Isthmus Slough). Error bars are provided in Supplemental Figs. S1–S8

exhibited a − 82% difference in accumulation rate. This site also coarsened through time, as did Brown's Cove, Crown Point, and East Flats 2.

SARs were greater than nearby RSLR rates in most cores for both timescales of averaging. For whole cores, SARs were 0.14 to 1.9 mm/yr greater than RSLR at all sites except East Flats 2 and Isthmus Slough (Table 2 column J). At these latter two sites, SARs were 0.49–0.57 mm/yr less than RSLR. For the 30-year timescale, SARs were 0.23 to 8.1 mm/yr greater than RSLR, and most values were at least 2 mm/yr greater than RSLR (Table 2 column K). The one exception was Charleston, where SAR was 0.48 mm/yr less than RSLR. It is worth noting that in all cases, (1) the RSLR value nearest to the core site was used (see Fig. 2B for location of RSLR estimates) and (2) the differences between SAR and RSLR exceeded the uncertainty in the corresponding SAR (Table 2).

Discussion

Spatial Variability in Accumulation Patterns

Time-averaged sediment and mass accumulation rates varied spatially across the estuary, both over long (1800s to present) and short (1990 to present) timescales (Table 2, Fig. 6). Over long timescales, SARs did not show any obvious spatial relationship to uplift rates or RSLR rates (Fig. 6B compared to Fig. 2), suggesting that SARs on intertidal flats are not strongly regulated by uplift rates or by RSLR.

Long-timescale SARs were 0.72–1.94 mm/yr greater than RSLR rates at most sites, with a few exceptions at the Charleston, East Flats 2, and Isthmus Slough sites (Fig. 6E, Table 2 column J). The Charleston core SAR was nearly equal to the local RSLR rate, suggesting that this tidal flat is effectively "keeping up" with sea-level rise. The East Flats 2 and Isthmus Slough cores exhibited SARs which were 0.49–0.57 mm/yr less than RSLR (Fig. 6E). Thus, over a centennial timescale, these two sites may be deepening (albeit at a very slow rate), though the reason is unknown. For example, deepening could be due to compaction, erosion, or insufficient sediment supply. Erosion is unlikely, however, because the surficial ^{210}Pb activities of those cores were not anomalously low compared with other sites, which would be an indicator of sediment removal.

The positive accretionary balance at most sites suggests that these locations have accommodation space available for sediment storage and are not net erosional and not sediment-supply-limited. This apparent infilling of the intertidal flats could represent one or more different processes—for example: (1) a natural, long-term positive accretionary balance driven by rates of sediment supply which exceed both rates of sediment removal and rates of compaction, in an environment which naturally has excess accommodation space; (2) infilling of new accommodation space created by subsidence during the 1700 earthquake (for reference, the estimated subsidence in South Slough was 0.85 m; Hawkes et al. 2011); and/or (3) a positive accretionary balance driven by increased sediment loads related to the logging (which peaked in the mid-1900s) and which may or may not persist into the future, given reductions in logging (Fig. 5B). All of these scenarios are plausible. For example, based on estimated SARs in South Slough of 1.2–2.1 mm/yr (Table 2 column E), in the ~ 320 years since the last major earthquake which caused 0.85 m of subsidence, 0.36–0.63 m of infilling should have occurred, assuming centennial rates can be extrapolated to 320 years. It is also possible that the system simply has excess capacity to store sediment and/or has seen an increase in sediment supply within the past century.

Mean SARs measured over shorter timescales (1990–present) exhibited similar spatial patterns as those measured over whole-core timescales (1800s to present), except that the lack of correlation with uplift/RSLR patterns was even more amplified in the more recent record. In other words, South Slough SARs were amplified within the last 30 years even more so than in the main estuary, despite this area experiencing the highest rates of uplift and lowest rates of RSLR rates (Table 2, Fig. 6C). This may reflect local processes of sediment trapping occurring in the relatively sheltered, undeveloped South Slough (see next section). Overall, these results from across the estuary further suggest that the system is not accommodation- or supply-limited.

It is worth noting that there was not a compelling relationship between SAR and water depth for either the long-term or short-term accretion rates (Tables 1 and 2). This was also observed by Brand et al. (in revision) for similar subtidal sites in Coos Bay, though they did observe a relationship between accretion and elevation in marshes higher in the tidal frame. All sites sampled in this study were located at > 0.5-m depth relative to mean sea level (based on bathymetry data from Conroy et al. 2020). The tidal-flat SARs observed here were generally greater than SARs observed on high marshes in other regional estuaries (Peck et al. 2020) as well as a high marsh-upland transition site sampled by Hawkes et al. (2011) at Crown Point in central South Slough—but higher accretion rates lower in the tidal frame may be a product of longer inundation times.

Temporal Variability in Accumulation Patterns—Evidence of Increased Sediment Supply/Retention, or Inter-decadal Sadler Effect?

Sediment accumulation rates are on the order of four times greater when averaged over the past 30 years versus centennial timescales at all sites except Charleston (Table 2, Figs. 5C-E, 6D, 7, and Figs. S4–S11). Note that Charleston

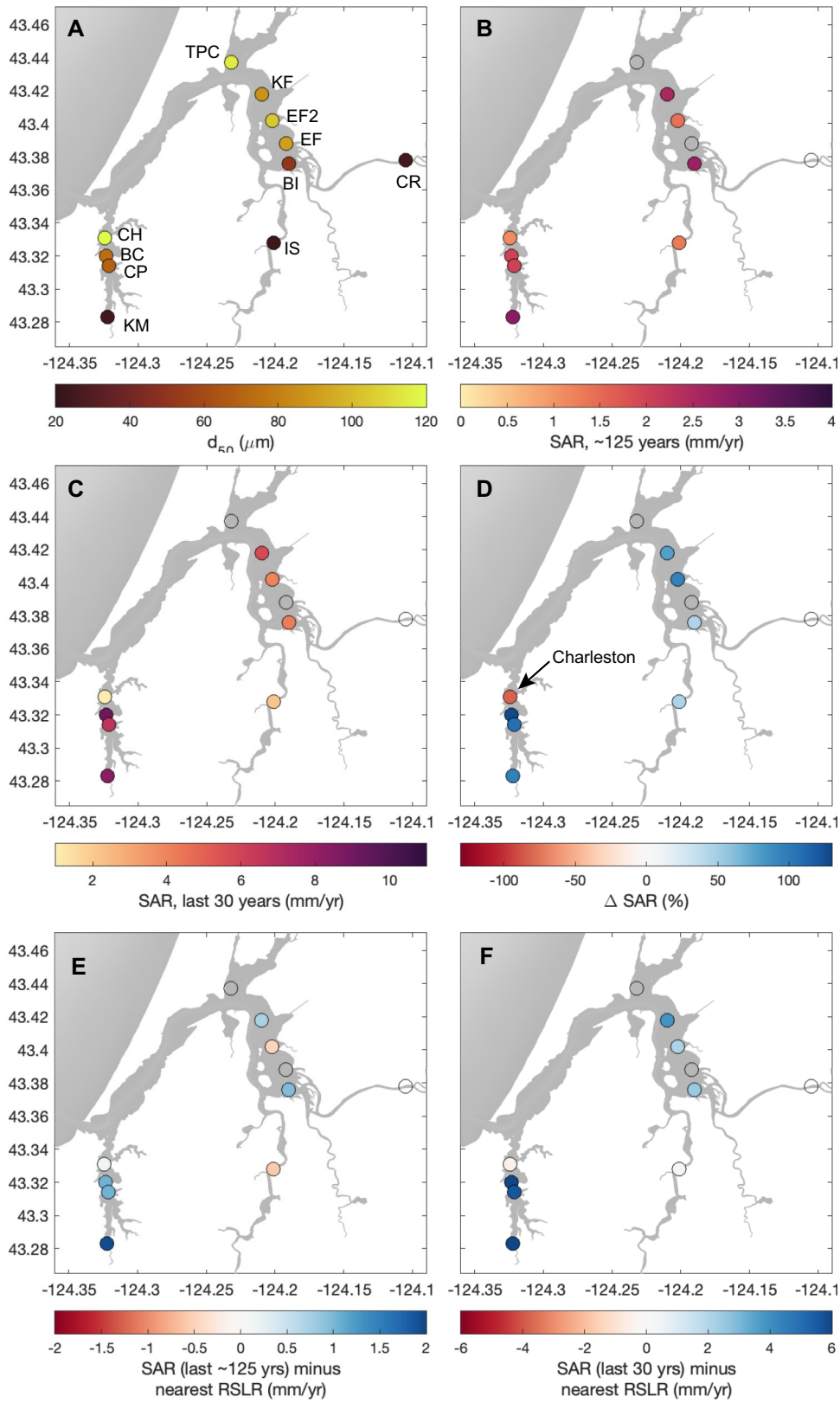

Fig. 6 Depth-averaged grain-size and SAR results. **A** Depth-averaged d_{50} for each core. Dark to light colors denote clay to sand, respectively. **B** Depth-averaged SAR for each core. **C** Depth-averaged SAR for the most recent 30-year record of each core. **D** Percent difference in SAR computed from the last 30 years of the core (**C**) versus the entire core (**B**). Blue colors (positive values) denote an increase in SAR over time, and red colors denote a decrease. **E** Difference between SAR averaged over the last ~125 years and the spatially nearest RSLR value (see Fig. 2B). Blue values denote SARs greater than RSLR and red values denote SARs less than RSLR. **F** Difference between SAR averaged over the last 30 years and the spatially nearest RSLR value. In all plots, empty circles denote cores not analyzed for isotopes/SARs due to excessive disturbance or very high sand fractions

is the site most distal to sediment sources, near an active harbor, and near active dredging—and thus may receive less sediment from rivers and experience more erosion from boat wakes and/or dredging, as evidenced by the slower modern SAR (relative to the long-term mean) and the slight coarsening through time (Fig. 3A). The apparent increases in

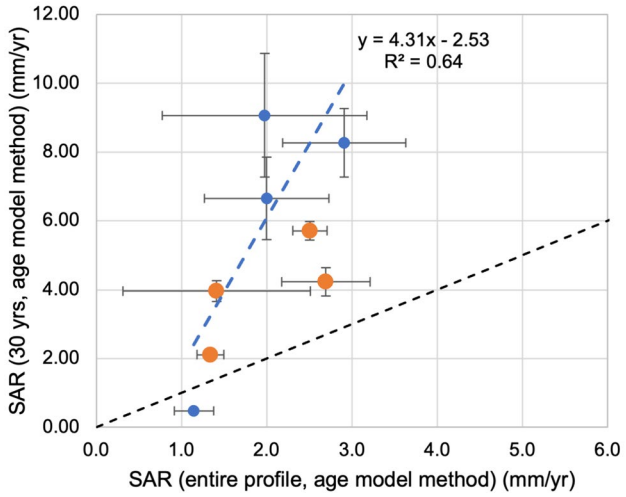

Fig. 7 Comparisons of SAR computed from the most recent 30 years of the core (column (F) in Table 2) versus SAR computed from the entire core (column (E) in Table 2). Smaller blue dots denote South Slough sites and larger orange dots denote Coos Bay sites

accretion observed at all other sites are manifest as increases in both background sediment accretion rates starting around the 1930s and the occurrence of peaks in accretion rates. Peaks are most prominent after 1990, and the largest peaks occur in South Slough (Fig. 5C, D). The presence of peaks only in the more recent records raises a question, however: do these results indicate real increases in sediment accretion, or an artifact of preservation versus mixing of peaks in isotope records?

It has been suggested that sediment supply to regional estuaries may have increased between the 1940s and 1970s due to enhanced precipitation during the wet phase of the Pacific Decadal Oscillation coupled with a rise in timber production (Peck and Wheatcroft 2022; Andrews and Kutara 2005; Fig. 5B). It is thus reasonable to conclude that SARs began increasing in Coos Bay around the 1960s with the highest peaks in the 1990s–present (Fig. 5C, D) as a result of increased sediment delivery. A lag between peak logging (1940s–1970s) and peak SARs (1990s to present) would not be surprising; changes in sediment delivery can lag landscape disturbances by years to decades owing to the time for root structures to decay and temporary storage of sediments within a watershed (e.g., Peck and Wheatcroft 2022; Noe et al. 2020).

Substantial development including dredging and intertidal flat reclamation also occurred in Coos Bay between 1910 and 1970, which reduced the total estuary area and increased the total volume (Ivy 2015; Borde et al. 2003; Eidam et al. 2020). Based on hydrodynamic and sediment-transport modeling, these changes led to an increase in estuarine circulation, a stronger estuarine turbidity maximum in the main navigation channel, and increased retention of sediment on intertidal flats, even in the absence of an increased sediment supply, which was not modeled (Eidam et al. 2020, 2021). This modeled increase in sediment retention is qualitatively consistent with the difference between the 30-year and whole-core mean SARs at most core sites (Fig. 6D), though the model results should not be overinterpreted since processes like waves, multi-decadal changes in weather patterns, and other non-stationary processes are not represented.

Effects of dredging and land reclamation should be less impactful in the protected South Slough Reserve, however, which makes the larger apparent increases in SAR here quite interesting. One theory for this enhanced accretion relative to the main estuary is that any logging which occurred in the Winchester Creek and neighboring watersheds could produce amplified signals of sediment accretion in South Slough because the subembayment is relatively sheltered and enclosed. In contrast, the main estuary has a large expanse of intertidal flats which likely experience stronger wave stresses and are drained by a larger network of channels.

A possible alternative explanation is that increases in SAR throughout the estuary are simply artifacts representing the Sadler effect (see Sadler 1981). This principle states that measured sediment accumulation rates will decrease in older portions of the sedimentary record as the length of a stratigraphic record increases, owing to an increasing number of hiatuses or erosional events which have impacted the record. In other words, sediment accretion rates are faster in the more modern part of the record without any real change in sediment delivery or trapping. This effect can be described by a power law, and can be identified through comparisons of SARs derived from geochronology methods suitable for different timescales, e.g., ^{210}Pb to represent a 100-year timescale and ^{14}C used to represent a 1000-year timescale (e.g., Sommerfield 2006; Rodriguez et al. 2020). This principle is supported by observations that monthly deposition rates can be an order of magnitude higher than centennial accumulation rates (e.g., McKee et al. 1983), though we are not aware of studies which have tried to quantify the Sadler effect per se over such short timescales.

While the Sadler effect is most often discussed in the context of longer-timescale records than those presented here, there are two lines of evidence which suggest that the apparent increases in SAR over the past 30–80 years may simply be artifacts in the data. First, the apparent increases in SAR post-1990 (or even post-1940s) are biased by sharp peaks in the datasets (Fig. 5C, D) which occur within 15 cm of the sediment surface (at most). That depth is generally within the range of bioturbation (e.g., Solan et al. 2019). In the Coos Bay cores, benthos were observed during core slicing, and it is reasonable to think there may be mixing to these depths. The recent peaks in SAR may thus be attenuated over time through mixing, leading to apparently lower

SARs similar to those interpreted in the older portions of the core records. Alternatively, other researchers have noted that bioturbation can bias SARs toward artificially high values by moving high-activity sediments downward in the profile—so the effect of bioturbation on SAR here is not clear without an independent measurement of mixing rates (Anderson et al. 1988). Furthermore, a companion study of short-timescale sediment accretion at these same core sites found monthly deposition or erosion values of up to 3 cm (Keogh et al. in revision), indicating a dynamic environment with centimeter-scale disturbance, and further suggesting that the SAR peaks observed here may be attenuated over time, and thus not represent any real increase in long-term SAR.

The second line of evidence suggesting the Sadler effect is in play is that when plotted on a semi-logarithmic scale, many of the age profiles can be reasonably described by a log-linear trend (Fig. S12), which is similar to the power-law nature of the Sadler effect. This similarity suggests that over time, sediment accretion rates converge to a low-magnitude background value in spite of perturbations that appear in the more recent record. In the absence of results from geochronology tools spanning different timescales (e.g., short-lived tracers for monthly to annual scales or ^{14}C for 1000-year timescales) as well as possible complications by tectonic uplift (i.e., non-stationarity in the system), it is not clear if the Sadler effect can be adequately quantified. However, this remains an interesting question for future research of seasonal to interdecadal estuarine sediment accretion, especially in light of present-day concerns about interdecadal sea-level rise.

Implications for Resiliency of Intertidal Environments in Terms of Vertical Accretion

For interpretations of estuarine resilience, sediment accretion rates are key because they provide information about whether a tidal flat may drown or keep pace with RSLR. Because of the labor and cost associated with coring and radiochemistry, estuary studies often have access to a limited number of cores for making these interpretations (with some notable exceptions—see Palinkas et al. 2013; Palinkas and Engelhardt 2015; and Peck et al. 2020 for examples of studies with high core density). The approaches used for constructing geochronologies also matter—for example, what is the relevant timescale of averaging accretion rates that should be used for projecting future trends? The results of this study thus have implications for studies of estuarine resilience in two areas: (1) by highlighting spatial variability of SARs (i.e., where do you choose to core to determine if an estuary is drowning, and how might interpretations be biased by a small number of cores?) and (2) by highlighting variability among the SAR results based on different timescales of averaging.

In terms of (1), it is interesting to note that SARs in this estuary varied spatially by a factor of two or more, with no clear relationship to distance from a source or water depth (Fig. S15). If a similar study was desired for a different estuary, what locations would make the "best" coring sites? For example, if the goal was to predict the overall stability of the intertidal flats (are they drowning or emerging?) or understand areas where maximum change is occurring, would it be better to core in the upper estuary, on the middle flats, or near the mouth? The results of this study show that this choice is complicated by varying spatial patterns of SARs. It is also important to note that subembayments like South Slough can behave differently from adjacent regions and may need to be evaluated separately.

For (2), the timescale of averaging for SARs impacts the results and interpretations. In this study, the more modern SARs were generally fourfold greater than the whole-core SARs (spanning a century or more; Fig. 7). This could represent a Sadler effect or could represent a real increase in sedimentation driven by a poorly constrained combination of factors (e.g., logging activity, increased precipitation, and/or changes in estuarine hydrodynamics). What values are most appropriate to use when making management decisions within the estuary? Over long timescales, sediments compact, erosion occurs, and SARs decrease to values that ultimately may be on par with RSLR. But over timescales of management decisions (e.g., decades), many of the intertidal areas in Coos Bay are accreting at rates far exceeding rates of relative sea-level rise, and thus, efforts to mitigate against submergence may be better directed elsewhere.

Conclusion

Sediment accumulation rates in the Coos Estuary vary spatially by a factor of two or more and have apparently increased through time. Rates generally exceed the rate of RSLR by 0.2–8 mm/yr, meaning the estuary is not accommodation-limited or supply-limited, and tidal flats (with the possible exception of the slow-accumulating sites of Charleston and Isthmus Slough) do not seem under threat of deeper submergence in the near future. These findings are consistent with work on high marshes (i.e., areas higher in the tidal frame) in other regional estuaries (Peck et al. 2020). Spatial variation in accretion shows a counterintuitive relation to uplift pattern: SARs are highest in South Slough where RSLR rates are lowest (with the exception of Charleston)—but this is not surprising because the system is not accommodation-limited. The reasons for spatial variations in SARs are not well-constrained, but it seems likely that amplification of accretion in South Slough may be because this subembayment is more sheltered and more effective at trapping sediment than the main estuary.

Within the past 30 years, sites with SARs > 2 mm/yr have preserved peaks in sediment accretion lasting a few years each. While no single cause can be absolutely linked to any of these patterns, it is reasonable to attribute these changes to increased precipitation and logging in the mid-1900s (see Andrews and Kutara 2005; Peck and Wheatcroft 2022) as well as hydrodynamic changes related to dredging and land reclamation (Eidam et al. 2021). It is also possible that these apparent increases represent a short-timescale Sadler effect, but over the timescales relevant to management decisions, using the higher accretion rates measured over the last few decades rather than the last century to interpret tidal flat resilience to sea-level rise seems appropriate.

Supplementary Information The online version contains supplementary material available at https://doi.org/10.1007/s12237-024-01407-x.

Acknowledgements We thank Dr. Brent McKee and Sherif Ghobrial (UNC Department of Earth, Marine, and Environmental Sciences) for their support of the geochronology lab work and helpful discussions about results. We also thank Daniela Zarate and Lillian Cooper for assistance processing cores and the South Slough NERRS team and UO volunteers for assisting with field collections. Finally, we thank two anonymous reviewers for their thoughtful comments which helped improve the manuscript.

Funding This work was sponsored by the National Estuarine Research Reserve System Science Collaborative, which supports collaborative research that addresses coastal management problems important to the reserves. The Science Collaborative is funded by the National Oceanic and Atmospheric Administration and managed by the University of Michigan Water Center (NA19NOS4190058). A description for this project is available at https://www.nerrssciencecollaborative.org/project/Sutherland20.

Data Availability All core data presented in this study are available in Eidam et al. 2023. All codes for applying classic age models to the ^{210}Pb activities have been made available in Matlab scripts hosted on GitHub (Souza 2022).

References

Anderson, R.F., R.F. Bopp, K.O. Buesseler, and P.E. Biscaye. 1988. Mixing of particles and organic constituents in sediments from the continental shelf and slope off Cape Cod: SEEP—I results. *Continental Shelf Research* 8 (5–7): 925–946.

Anderson, R.O. 2020. High resolution remote sensing of eelgrass (Zostera marina) in South Slough, Oregon (M.S.). University of Oregon, United States -- Oregon. Retrieved from https://search.proquest.com/docview/2436877847/abstract/40CA2C1D0E814277PQ/1.

Andrews, A., & Kutara, K. (2005). Oregon's timber harvests: 1849–2005. Oregon Department of Forestry. https://www.oregon.gov/odf/Documents/workingforests/oregonstimberharvests.pdf.

Appleby, P.G. 2008. Three decades of dating recent sediments by fallout radionuclides: A review. *The Holocene* 18 (1): 83–93.

Appleby, P.G., and F. Oldfield. 1978. The calculation of lead-210 dates assuming a constant rate of supply of unsupported ^{210}Pb to the sediment. *CATENA* 5 (1): 1–8.

Appleby, P.G. 2001. Chronostratigraphic techniques in recent sediments. In *Tracking environmental change using lake sediments: basin analysis, coring, and chronological techniques*, ed. W.M. Last and J.P. Smol, 171–203. Dordrecht: Springer Netherlands. https://doi.org/10.1007/0-306-47669-X_9.

Arias-Ortiz, A., P. Masqué, J. Garcia-Orellana, O. Serrano, I. Mazarrasa, N. Marbà, and C.M. Duarte. 2018. Reviews and syntheses: 210 Pb-derived sediment and carbon accumulation rates in vegetated coastal ecosystems–setting the record straight. *Biogeosciences* 15 (22): 6791–6818.

Boldt, K.V., C.A. Nittrouer, and A.S. Ogston. 2013. Seasonal transfer and net accumulation of fine sediment on a muddy tidal flat: Willapa Bay, Washington. *Continental Shelf Research* 60: S157–S172.

Borde, A.B., R.M. Thom, S. Rumrill, and L.M. Miller. 2003. Geospatial habitat change analysis in Pacific Northwest coastal estuaries. *Estuaries* 26 (4): 1104–1116. https://doi.org/10.1007/BF02803367.

Brand, M.W., Cornu, C., Diefenderfer, H.L., Janousek, C., Borde, A.B., Souza, T., Keogh, M., Bridgham, S. (in revision). Thresholds for reducing nuisance flooding under sea-level rise using wetland restoration. Water Resources Research.

Breda, A., P.M. Saco, S.G. Sandi, N. Saintilan, G. Riccardi, and J.F. Rodríguez. 2021. Accretion, retreat and transgression of coastal wetlands experiencing sea-level rise. *Hydrology and Earth System Sciences* 25 (2): 769–786. https://doi.org/10.5194/hess-25-769-2021.

Brush, G.S., E.A. Martin, R.S. DeFries, and C.A. Rice. 1982. Comparisons of 210Pb and pollen methods for determining rates of estuarine sediment accumulation. *Quaternary Research* 18 (2): 196–217.

Burgette, R.J., R.J. Weldon II., and D.A. Schmidt. 2009. Interseismic uplift rates for western Oregon and along-strike variation in locking on the Cascadia subduction zone. *Journal of Geophysical Research: Solid Earth*. https://doi.org/10.1029/2008JB005679.

Carpenter, R., J.T. Bennett, and M.L. Peterson. 1981. 210Pb activities in and fluxes to sediments of the Washington continental slope and shelf. *Geochimica Et Cosmochimica Acta* 45 (7): 1155–1172. https://doi.org/10.1016/0016-7037(81)90139-3.

Conroy, T., D.A. Sutherland, and D.K. Ralston. 2020. Estuarine exchange flow variability in a seasonal, segmented estuary. *Journal of Physical Oceanography* 50 (3): 595–613. https://doi.org/10.1175/JPO-D-19-0108.1.

Eidam, E.F., D.A. Sutherland, D.K. Ralston, B. Dye, T. Conroy, J. Schmitt, et al. 2020. Impacts of 150 years of shoreline and bathymetric change in the Coos Estuary, Oregon, USA. *Estuaries and Coasts*. https://doi.org/10.1007/s12237-020-00732-1.

Eidam, E.F., D.A. Sutherland, D.K. Ralston, T. Conroy, and B. Dye. 2021. Shifting sediment dynamics in the Coos Estuary in response to 150 years of modification. *Journal of Geophysical Reseach: Oceans*. https://doi.org/10.1029/2020JC016771.

Eidam, E.F.; Souza, T.; Keogh, M.; Sutherland, D.; Schmitt, J.; Helms, A. (2023). Sediment grain size, organic content, and Pb-210 excess activity in Coos Bay from 2021–05–17 to 2021–05–19 (NCEI Accession 0277842). NOAA National Centers for Environmental Information. Dataset. https://doi.org/10.25921/ywjy-3f15. Accessed September 19, 2023.

Groth, S., and S. Rumrill. 2009. History of Olympia oysters (Ostrea lurida Carpenter 1864) in Oregon estuaries, and a description of recovering populations in Coos Bay. *Journal of Shellfish Research* 28 (1): 51–58. https://doi.org/10.2983/035.028.0111.

Gunnell, J.R., A.B. Rodriguez, and B.A. McKee. 2013. How a marsh is built from the bottom up. *Geology* 41 (8): 859–862. https://doi.org/10.1130/G34582.1.

Hawkes, A.D., B.P. Horton, A.R. Nelson, C.H. Vane, and Y. Sawai. 2011. Coastal subsidence in Oregon, USA, during the giant Cascadia earthquake of AD 1700. *Quaternary Science Reviews* 30 (3): 364–376. https://doi.org/10.1016/j.quascirev.2010.11.017.

He, Q., and D.E. Walling. 1996. Interpreting particle size effects in the adsorption of 137Cs and unsupported ^{210}Pb by mineral soils and sediments. *Journal of Environmental Radioactivity* 30 (2): 117–137.

Holmquist, J.R., L. Windham-Myers, N. Bliss, S. Crooks, J.T. Morris, J.P. Megonigal, and M. Woodrey. 2018. Accuracy and precision of tidal wetland soil carbon mapping in the conterminous United States. *Scientific Reports* 8 (1): 9478.

Ivy, D. (2015). A very brief overview of the Coos Bay area's economic and cultural history. Retrieved December 3, 2020, from http://www.partnershipforcoastalwatersheds.org/wordpress/wp-content/uploads/2015/08/CommCultural-History-Chapter-08142015.pdf.

Johnson, G.M., D.A. Sutherland, J.J. Roering, N. Mathabane, and D.G. Gavin. 2019. Estuarine dissolved oxygen history inferred from sedimentary trace metal and organic matter preservation. *Estuaries and Coasts* 42 (5): 1211–1225. https://doi.org/10.1007/s12237-019-00580-8.

Keogh, M., D. Sutherland, E. Eidam, T. Souza, J. Schmitt, A. Helms, D.K. Ralston. in revision. Estuarine sediment dynamics and the importance of storms in moving mud. *Estuaries and Coasts*.

Kirwan, M.L., and J.P. Megonigal. 2013. Tidal wetland stability in the face of human impacts and sea-level rise. *Nature* 504 (7478): 53–60. https://doi.org/10.1038/nature12856.

Krishnaswamy, S., D. Lal, J.M. Martin, and M. Meybeck. 1971. Geochronology of lake sediments. *Earth and Planetary Science Letters* 11 (1–5): 407–414.

Maddin, I. P. 1995. Geologic map of Coos Bay Quadrangle. USGS. Retrieved from https://www.oregongeology.org/pubs/gms/GMS-097.pdf.

Mathabane, N. 2015. Potential impacts of timber harvesting, climate, and conservation on sediment accumulation and dispersal in the South Slough National Estuarine Reserve, OREGON, 44.

McKee, B.A., C.A. Nittrouer, and D.J. DeMaster. 1983. Concepts of sediment deposition and accumulation applied to the continental shelf near the mouth of the Yangtze River. *Geology* 11 (11): 631–633.

Nelson, A.R., Y. Ota, M. Umitsu, K. Kashima, and Y. Matsushima. 1998. Seismic or hydrodynamic control of rapid late-Holocene sea-level rises in southern coastal Oregon, USA? *The Holocene* 8 (3): 287–299.

Nittrouer, C.A., R.W. Sternberg, R. Carpenter, and J.T. Bennett. 1979. The use of Pb-210 geochronology as a sedimentological tool: Application to the Washington continental shelf. *Marine Geology* 31 (3): 297–316. https://doi.org/10.1016/0025-3227(79)90039-2.

NOAA. 2022. Sea level trends - NOAA tides & currents. Retrieved August 22, 2023, from https://tidesandcurrents.noaa.gov/sltrends/sltrends_station.shtml?id=9432780.

Noe, G.B., M.J. Cashman, K. Skalak, A. Gellis, K.G. Hopkins, D. Moyer, et al. 2020. Sediment dynamics and implications for management: State of the science from long-term research in the Chesapeake Bay watershed, USA. *Wires Water* 7 (4): e1454. https://doi.org/10.1002/wat2.1454.

Palinkas, C.M., K.A. Engelhardt, and D. Cadol. 2013. Evaluating physical and biological influences on sedimentation in a tidal freshwater marsh with 7Be. *Estuarine, Coastal and Shelf Science* 129: 152–161.

Palinkas, C., and K.A.M. Engelhardt. 2015. Spatial and temporal patterns of modern (~100 yr) sedimentation in a tidal freshwater marsh: implications for future sustainability. Limnology and Oceanography - Wiley Online Library. Retrieved October 14, 2021, from https://aslopubs.onlinelibrary.wiley.com/doi/full/10.1002/lno.10202.

Peck, E.K., R.A. Wheatcroft, and L.S. Brophy. 2020. Controls on sediment accretion and blue carbon burial in tidal saline wetlands: insights from the Oregon Coast, USA. *Journal of Geophysical Research: Biogeosciences* 125 (2): e2019JG005464. https://doi.org/10.1029/2019JG005464.

Peck, E.K., and R.A. Wheatcroft. 2022. Spatiotemporal variation in Oregon salt marsh expansion and contraction. *Estuarine, Coastal and Shelf Science* 273: 107908.

Percy, K., D. Bella, C. Sutterlin, and P. Klingeman. 1974. Descriptions and information sources for Oregon estuaries. Retrieved June 17, 2022, from https://onlinebooks.library.upenn.edu/webbin/book/lookupid?key=ha007248871.

Port of Coos Bay, P. 2018. What's going down in the timber industry? Retrieved June 6, 2022, from https://www.portofcoosbay.com/new-room/2018/11/2/whats-going-down-in-the-timber-industry.

Robbins, J.A. (1978). Geochemical and geophysical applications of radioactive lead. Biogeochemistry of Lead in the Environment, 285–393.

Rodriguez, A.B., B.A. McKee, C.B. Miller, M.C. Bost, and A.N. Atencio. 2020. Coastal sedimentation across North America doubled in the 20th century despite river dams. *Nature Communications* 11 (1): 3249. https://doi.org/10.1038/s41467-020-16994-z.

Rumrill, S.S., and D.C. Sowers. 2008. Concurrent assessment of eelgrass beds (Zostera marina) and salt marsh communities along the estuarine gradient of the South Slough. *Oregon. Journal of Coastal Research* 2008 (10055): 121–134. https://doi.org/10.2112/SI55-016.1.

Rumrill, S. S. (2007). *Site profile of the South Slough National Estuarine Research Reserve* (Technical Report) (p. 258). Charleston, OR: South Slough National Estuarine Research Reserve.

Sadler, P.M. 1981. Sediment accumulation rates and the completeness of stratigraphic sections. *The Journal of Geology* 89 (5): 569–584.

Saldías, G.S., P.T. Strub, and R.K. Shearman. 2020. Spatio-temporal variability and ENSO modulation of turbid freshwater plumes along the Oregon coast. *Estuarine, Coastal and Shelf Science* 243: 106880. https://doi.org/10.1016/j.ecss.2020.106880.

Sanchez-Cabeza, J.A., and A.C. Ruiz-Fernández. 2012. 210Pb sediment radiochronology: An integrated formulation and classification of dating models. *Geochimica Et Cosmochimica Acta* 82: 183–200.

Solan, M., E.R. Ward, E.L. White, E.E. Hibberd, C. Cassidy, J.M. Schuster, and J.A. Godbold. 2019. Worldwide measurements of bioturbation intensity, ventilation rate, and the mixing depth of marine sediments. *Scientific Data* 6 (1): 58.

Sommerfield, C.K. 2006. On sediment accumulation rates and stratigraphic completeness: Lessons from Holocene ocean margins. *Continental Shelf Research* 26 (17–18): 2225–2240.

Souza, T. (2022). Processing Lead-210 (Pb-210) Alpha spectrometry data for geochronology. MATLAB. Retrieved from https://github.com/tsouza96/processing_lead_210_sediment_data on 13 October, 2022.

Thorne, K., G. MacDonald, G. Guntenspergen, R. Ambrose, K. Buffington, B. Dugger, et al. 2018. U.S. Pacific coastal wetland resilience and vulnerability to sea-level rise. *Science Advances*. https://doi.org/10.1126/sciadv.aao3270.

United States Army Corps of Engineers (USACE). 2015. Environmental assessment: Coos Bay maintenance dredging. *CoosBay2015EAandFONSI.Pdf*. Retrieved from https://erdc-library.erdc.dren.mil/jspui/handle/11681/18580.

van Dijk, W.M., J.R. Cox, J.R.F.W. Leuven, J. Cleveringa, M. Taal, M.R. Hiatt, et al. 2021. The vulnerability of tidal flats and multichannel estuaries to dredging and disposal. *Anthropocene Coasts* 4 (1): 36–60. https://doi.org/10.1139/anc-2020-0006.

Zaborska, A., J. Carroll, C. Papucci, and J. Pempkowiak. 2007. Intercomparison of alpha and gamma spectrometry techniques used in 210PB geochronology. *Journal of Environmental Radioactivity* 93 (1): 38–50. https://doi.org/10.1016/j.jenvrad.2006.11.007.

Zhang, Y., and B. Xu. 2023. Fidelity of the 210Pb dating method, a subaquatic sediment perspective. *Science of the Total Environment* 871: 161972.

Zhang, F., J. Wang, M. Baskaran, Q. Zhong, Y. Wang, J. Paatero, and J. Du. 2021. A global dataset of atmospheric ^{7}Be and ^{210}Pb measurements: Annual air concentration and depositional flux. *Earth System Science Data* 13 (6): 2963–2994. https://doi.org/10.5194/essd-13-2963-2021.